

An Underwater Image Enhancement Benchmark Dataset and Beyond

Chongyi Li, Chunle Guo, Wenqi Ren, Runmin Cong, Junhui Hou,
Sam Kwong, *Fellow, IEEE*, and Dacheng Tao, *Fellow, IEEE*

Abstract—Underwater image enhancement has been attracting much attention due to its significance in marine engineering and aquatic robot. Numerous underwater image enhancement algorithms have been proposed in the last few years. However, these algorithms are mainly evaluated using either synthetic datasets or few selected real-world images. It is thus unclear how these algorithms would perform on images acquired in the wild and how we could gauge the progress in the field. To bridge this gap, we present the first comprehensive perceptual study and analysis of underwater image enhancement using large-scale real-world degraded images. In this paper, we construct an *Underwater Image Enhancement Benchmark Dataset (UIEBD)* including 950 real-world underwater images, 890 of which have the corresponding reference images. We treat the rest 60 underwater images which cannot obtain satisfactory references as challenging data. Using this dataset, we conduct a comprehensive study of the state-of-the-art underwater image enhancement algorithms qualitatively and quantitatively. In addition, we propose an end-to-end Deep Underwater Image Enhancement Network (DUIENet) trained on this benchmark as a baseline, which indicates the generalization of the proposed UIEBD for training Convolutional Neural Networks (CNNs). The benchmark evaluations and the proposed DUIENet demonstrate the performance and limitations of state-of-the-art algorithms which shed light on the future research in underwater image enhancement. The code and dataset are available at: https://li-chongyi.github.io/homepage.github.io/proj_benchmark.html

Index Terms—underwater image enhancement, real-world underwater images, comprehensive evaluation, deep learning.

I. INTRODUCTION

DURING the past few years, underwater image enhancement has drawn considerable attention in both image processing and computer vision [1], [2]. Due to the complicated underwater environment and lighting conditions, enhancing underwater image is a challenging problem. Usually,

This work was supported in part by the National Natural Science Foundation of China under Grant 61771334 (*Corresponding author: Wenqi Ren*)

Chongyi Li, Junhui Hou, and Sam Kwong are with the Department of Computer Science, City University of Hong Kong, Kowloon, Hong Kong, China (e-mail: lichongyi25@gmail.com; jh.hou@cityu.edu.hk; cssamk@cityu.edu.hk).

Chunle Guo is with the School of Electrical and Information Engineering, Tianjin University, Tianjin, China (e-mail: guochunle@tju.edu.cn).

Wenqi Ren is with State Key Laboratory of Information Security, Institute of Information Engineering, Chinese Academy of Sciences, China (e-mail: rwq.renwenqi@gmail.com).

Runmin Cong is with the School of Electrical and Information Engineering, Tianjin University, Tianjin, China, and also with the Department of Computer Science, City University of Hong Kong, Kowloon, Hong Kong, China (e-mail: runmincong@gmail.com).

Dacheng Tao is with the UBTECH Sydney Artificial Intelligence Centre and the School of Information Technologies, the Faculty of Engineering and Information Technologies, the University of Sydney, 6 Cleveland St, Darlington, NSW 2008, Australia (e-mail: dacheng.tao@sydney.edu.au).

an underwater image is degraded by wavelength-dependent absorption and scattering including forward scattering and backward scattering [3]–[7]. In addition, the marine snow introduces noise and increases the effects of scattering. These adverse effects reduce visibility, decrease contrast, and even introduce color casts, which limits the practical applications of underwater images and videos in marine biology and archaeology [8], marine ecological [9], to name a few. To solve this problem, earlier methods rely on multiple underwater images or polarization filters, while recent algorithms deal with this problem by using only information from a single image.

Despite the prolific work, both the comprehensive study and insightful analysis of underwater image enhancement algorithms remain largely unsatisfactory due to the lack of a publicly available real-world underwater image dataset. Additionally, lacking sufficient and effective training data, the performance of deep learning-based underwater image enhancement algorithms does not match the success of recent deep learning-based high-level [10], [11] and low-level [12], [13] vision problems. To advance the development of underwater image enhancement, we construct a large-scale real-world *Underwater Image Enhancement Benchmark Dataset (UIEBD)*. Several sampling images and the corresponding reference images from UIEBD are presented in Fig. 1. As shown, the raw underwater images in the UIEBD have diverse color ranges and degrees of contrast decrease. In contrast, the corresponding reference results are color casts-free (at least relatively genuine color) and have improved visibility and brightness. With the proposed UIEBD, we carry out a comprehensive study for several state-of-the-art single underwater image enhancement algorithms both qualitatively and quantitatively, which enables insights into their performance and sheds light on the future research. In addition, with the constructed UIEBD, CNNs can be easily trained to improve the visual quality of an underwater image. To demonstrate this application, we propose an underwater image enhancement CNN model trained by the proposed UIEBD.

The main contributions of this paper are summarized as follows:

- We construct a large-scale real-world underwater image enhancement benchmark dataset (*i.e.*, **UIEBD**) which contains 950 degraded underwater images. Moreover, the corresponding reference results for 890 images are provided according to laborious, time-consuming, and well-designed pairwise comparisons. UIEBD provides a platform to evaluate, at least to some extent, the performance of different underwater image enhancement



Fig. 1. Sampling images from the constructed UIEBD. Top row: raw underwater images taken in diverse underwater scenes; Bottom row: the corresponding reference results.

algorithms. It also makes strongly supervised underwater image enhancement models which are out of the constraints of specific underwater scenes possible.

- With the constructed UIEBD, we conduct a comprehensive study of the state-of-the-art single underwater image enhancement algorithms ranging from qualitative to quantitative evaluations. Our evaluations and analyses provide comprehensive insights into the strengths and limitations of current underwater image enhancement algorithms, and suggest new research directions.
- We propose a CNN model (*i.e.*, **DUIENet**) trained by the constructed UIEBD for underwater image enhancement, which demonstrates the generalization of the constructed UIEBD and the advantages of our DUIENet, and also motivates the development of deep learning-based underwater image enhancement.

II. EXISTING METHODOLOGY, EVALUATION METRIC, AND DATASET: AN OVERVIEW

A. Underwater Image Enhancement Method

Exploring underwater world has become an active issue in recent years [14]–[16]. Underwater image enhancement as an indispensable step to improve the visual quality of recorded images has drawn much attention. A variety of methods have been proposed and can be organized into four groups: supplementary information-based methods, non-physical model-based methods, physical model-based methods, and data-driven methods.

Supplementary information-based methods: In the earlier stage, supplementary information from multiple images [17] or specialize hardware devices (*e.g.*, polarization filtering [18]–[21], range-gated imaging [22], [23], and fluorescence imaging [24], [25]) were utilized to improve the visibility of underwater images. Compared to supplementary information-based methods, single underwater image enhancement has been proven to be more suitable for challenging situations such as dynamic scenes, and thus, gains extensive attention.

Non-physical model-based methods: Non-physical model-based methods aim to modify image pixel values to improve the visual quality. Iqbal *et al.* [26] stretched the dynamic pixel range in RGB color space and HSV color space to improve the contrast and saturation of an underwater image. Chani and Isa

[27], [28] modified the work of [26] to reduce the over/under-enhanced regions by shaping the stretching process following the Rayleigh distribution. Ancuti *et al.* [29] proposed an underwater image enhancement method by blending a contrast-enhanced image and a color-corrected image in a multi-scale fusion strategy. In [30], a two-step approach for underwater image enhancement was proposed, which includes a color correction algorithm and a contrast enhancement algorithm.

Another line of research tries to enhance underwater images based on the Retinex model. Fu *et al.* [31] proposed a Retinex-based method for underwater image enhancement, which consists of color correction, layer decomposition, and enhancement. Zhang *et al.* [32] proposed an extended multi-scale Retinex based underwater image enhancement method. In this work, it is interesting that the underwater turbidity conditions are simulated by using a mixture of whole milk and grape juice in the water.

Physical model-based methods: Physical model-based methods regard the enhancement of an underwater image as an inverse problem, where the latent parameters of an underwater image formation model are estimated from input image. These methods usually follow the same pipeline: 1) building a physical model of the degradation; 2) estimating the unknown model parameters; and 3) addressing this inverse problem.

One line of research is to modify the Dark Channel Prior (DCP) [33] for underwater image enhancement. In [34], DCP was combined with the wavelength-dependent compensation algorithm to restore the underwater image. In [35], an Underwater Dark Channel Prior (UDCP) was proposed based on the fact that the information of the red channel in an underwater image is undependable. Based on the observation that the dark channel of the underwater image tends to be a zero map, Liu and Chau [36] formulated a cost function and minimized it so as to find the optimal transmission map which is able to maximize the image contrast. Instead of the DCP, Li *et al.* [37] employed the random forest regression model to estimate the medium transmission of the underwater scenes. Recently, Peng *et al.* [38] proposed a Generalized Dark Channel Prior (GDCP) for image restoration, which incorporates adaptive color correction into an image formation model.

Another line of research is to employ the optical properties of underwater imaging. Carlevaris-Bianca *et al.* [39] proposed

a prior that exploits the difference in attenuation among three color channels in RGB color space to predict the medium transmission of an underwater scene. The idea behind this prior is that the red light usually attenuates faster than the green light and the blue light in an underwater scenario. Galdran *et al.* [40] proposed a Red Channel method, which recovers the lost contrast of an underwater image by restoring the colors associated with short wavelengths. According to the findings that the background color of underwater images has relations with the inherent optical properties of water medium, Zhao *et al.* [41] enhanced the degraded underwater images by deriving inherent optical properties of water from the background color. Li *et al.* [42] proposed an underwater image enhancement method based on the minimum information loss principle and histogram distribution prior. Peng *et al.* [43] proposed a depth estimation method for underwater scenes based on image blurriness and light absorption, which is employed in an underwater image formation model to enhance underwater images. Berman *et al.* [44] took multiple spectral profiles of different water types into account and reduced the problem of underwater image restoration to single image dehazing by estimating two additional global parameters. Wang *et al.* [45] combined the adaptive attenuation-curve prior with the characteristics of underwater light propagation for underwater image restoration.

Data-driven methods: Recent years have witnessed significant advance of deep learning in low-level vision problems, including image super-resolution [46]–[48], image denoising [49], [50], image deblurring [51], [52], image dehazing [53], [54], *etc.* These methods can be trained using synthetic pairs of degraded images and high-quality counterparts. However, underwater image formation models depend on specific scenes and lighting conditions, and even are related to temperature and turbidity. Thus, it is difficult to synthesize realistic underwater images for CNN training. Further, the learned distribution by CNN trained on synthetic underwater images does not always generalize to the real-world underwater images. Therefore, the performance and the amount of deep learning-based underwater image enhancement methods do not match the success of recent deep learning-based low-level vision problems due to the lack of sufficient and effective training data.

Recently, Li *et al.* [55] proposed a deep learning-based underwater image enhancement model, called WaterGAN. WaterGAN first simulates realistic underwater images from the in-air image and depth pairings in an unsupervised pipeline. With the synthetic training data, the authors use a two-stage network for underwater image restoration, especially for color casts removal. However, the testing data are similar to the training data since the generalization of the WaterGAN is limited due to the training data simulated in specific scenes. More recently, a weakly supervised underwater color transfer model [56] was proposed based on Cycle-Consistent Adversarial Networks [57]. Benefiting from the adversarial network architecture and multiterm loss function, this network model relaxes the need for paired underwater images for training and allows the underwater images being taken in unknown locations. However, it tends to produce inauthentic results in some

cases due to the nature of multiple possible outputs. In [58], Hou *et al.* synthesized underwater images by setting random parameters of an underwater image formation using the prior of wavelength-dependent attenuation and developed an underwater residual CNN model to learn the transmission. However, the employed underwater image formation cannot hold well in real cases. Therefore, the robustness and generalization of deep learning-based underwater enhancement methods still fall behind conventional state-of-the-art algorithms.

B. Underwater Image Quality Evaluation

Different from other low-level vision problems where the ground truth can be easily obtained (*e.g.*, image super-resolution), it is challenging to achieve a large amount of paired degraded underwater images and the corresponding ground truth. In the following, we will give a brief introduction of the image quality evaluation metrics which are usually used for the performance evaluation of underwater image enhancement methods.

Full-reference metrics: For an underwater image with ground truth, the full-reference image quality evaluation metrics (*e.g.*, MSE, PSNR, and SSIM [59]) were employed for evaluation. Such underwater images usually are a few color checker images or color image patches taken in the simulated or real underwater environment. For example, Zhao *et al.* [41] treated a plastic color disk as ground truth and captured its underwater image in a water pool as the testing image.

Non-reference metrics: For a real-world underwater image where the ground truth was unavailable, non-reference image quality evaluation metrics, such as image entropy, visible edges [60], dynamic range independent image quality assessment [61], were utilized. In addition, some authors employed specific applications, like feature point matching, edge detection, and image segmentation, to evaluate their results. Recently, several specific non-reference metrics were proposed for underwater images evaluation. Yang and Sowmya [62] proposed an underwater color image quality evaluation metric (*i.e.*, UCIQE). UCIQE first quantifies the non-uniform color casts, blurring, and low contrast, and then combines these three components in a linear manner, which has been widely used. In [63], the authors proposed a non-reference underwater image quality measure, called UIQM, which comprises three attribute measures: a colorfulness measure, a sharpness measure, and a contrast measure. Each presented attribute measure is inspired by the properties of the human visual system.

C. Underwater Image Dataset

There are several real-world underwater image datasets such as Fish4Knowlege dataset for underwater target detection and recognition¹, underwater images in SUN dataset for scene recognition and object detection² [64], and MARIS dataset for marine autonomous robotics³. However, existing datasets are not suitable for the enhancement task due to the monotonous

¹<http://groups.inf.ed.ac.uk/f4k/>

²<http://groups.csail.mit.edu/vision/SUN/>

³<http://rimlab.ce.unipr.it/Marisi.html>

content and limited scenes, few degradation characteristics, and insufficient data. Besides, to synthesize underwater images, Li *et al.* [55] proposed a GAN based method while Duarte *et al.* [65] simulated underwater image degradation using milk, chlorophyll, or green tea in a tank. Blasinski *et al.* [66] provided an open-source underwater image simulation tool and a three parameter underwater image formation model [67]. However, there still exists a gap between the synthetic and real-world underwater images. Therefore, it is difficult to evaluate the state-of-the-art underwater image enhancement methods fairly and comprehensively, and is hard to develop effective deep learning-based underwater image enhancement models without reference images.

III. PROPOSED BENCHMARK DATASET

After systematically reviewing previous work, we found the main issue existing in the community of underwater image enhancement is lacking a large-scale real-world underwater image dataset with reference images. In what follows, we introduce the constructed dataset in detail, including data collection and reference image generation.

A. Data Collection

There are three objectives for underwater image collection:

- 1) a diversity of underwater scenes, different characteristics of quality degradation, and a broad range of image content should be covered;
- 2) the amount of degraded underwater images should be large; and
- 3) the corresponding high-quality reference images should be provided so that pairs of images enable fair image quality evaluation and end-to-end learning.

To achieve the first two objectives, we first collect a large number of underwater images, and then refine them. We mainly retain the underwater images which meet the first objective. After data refinement, most of the collected images are weeded out, and about 950 candidate images are remaining. The resolution of the remaining images ranges from 183×275 to 1350×1800 . Fig. 2 gives some examples of the images in the conducted UIEBD. It is almost impossible to achieve the ground truth of the collected underwater images. To achieve the third objective, we introduce a high-quality reference image generation method in the next section.

B. Reference Image Generation

With the candidate underwater images, the potential reference images are generated by 12 image enhancement methods, including 9 underwater image enhancement methods (*i.e.*, Fusion-based [29], Two-step-based [30], Retinex-based [31], UDCP [35], Regression-based [37], GDPC [38], Red Channel [40], Histogram Prior [42], and Blurriness-based [43]), 2 image dehazing methods (*i.e.*, DCP [33] and MSCNN [53]), and 1 commercial application for enhancing underwater images (*i.e.*, dive+⁴). We exclude the recent deep learning-based methods due to their limited generalization capability to the diverse



Fig. 2. Examples of the images in the conducted UIEBD. These images have obvious characteristics of underwater image quality degradation (*e.g.*, color casts, decreased contrast, and blurring details) and are taken in a diversity of underwater scenes.

real-world underwater images. All the employed methods except the fusion-based [29] method are realized by the source codes provided by their authors. We reimplement the fusion-based [29] method since the source code is unavailable. For the dive+, we tune its parameter settings to generate satisfactory results. At last, we totally generate 12×950 enhanced results.



Fig. 3. An example of pair comparisons. Treating the raw underwater image as reference, a volunteer needs to independently decide which one is better between the results of method A and method B.

With raw underwater images and the enhanced results, we invite 50 volunteers (25 volunteers with image processing experience; 25 volunteers without related experience) to perform pairwise comparisons among the 12 enhanced results of each raw underwater image under the same monitor. The pairwise comparisons have been proven to be more robust and consistent in subjective perception than individual rating [68], [69], though it is laborious and time-consuming.

Specifically, each volunteer is shown a raw underwater image and a set of enhanced result pairs. The enhanced image pairs are drawn from all the competitive methods randomly, and the result winning the pairwise comparisons will be compared again in the next round, until the best one is selected. There is no time constraint for volunteers and zoom-in operation is allowed. An example of pair comparisons is shown in Fig. 3. For each pair of enhanced results, taking the raw underwater image as reference, a volunteer first needs to independently decide which one is better than the other. Therefore, for each volunteer, the best result of a raw underwater image

⁴<https://itunes.apple.com/us/app/dive-video-color-correction/id1251506403?mt=8>

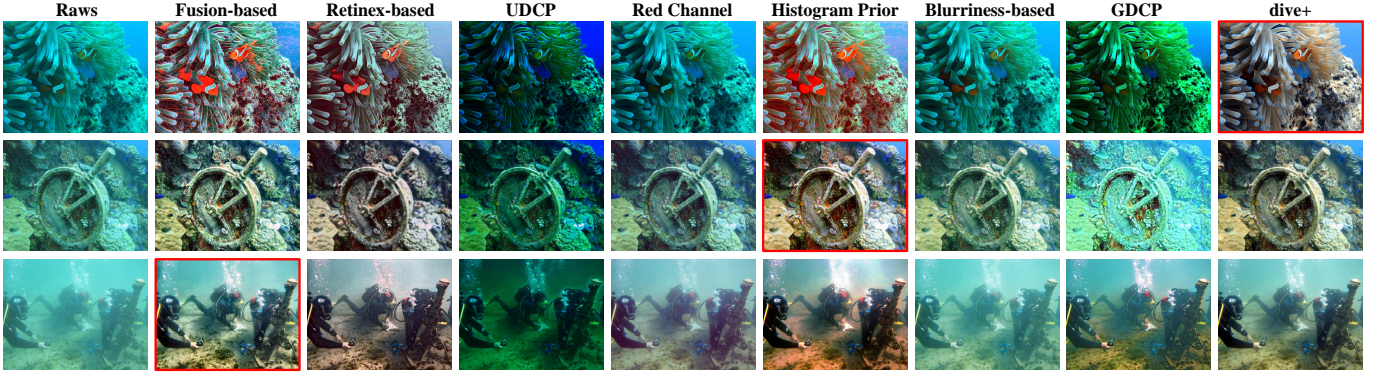


Fig. 4. Results generated by different methods. From left to right are raw underwater images, and the results of Fusion-based [29], Retinex-based [31], UDCP method [35], Red Channel [40], Histogram Prior [42], Blurriness-based [43], GDCP [38] and dive+. Red boxes indicate the final reference images.

will be selected after 11 pair comparisons. In addition, the volunteer needs to inspect the best result again and then label the best result as being satisfactory or dissatisfactory. At last, the reference image for a raw underwater image is first selected by majority voting after pair comparisons. After that, if the selected reference image has greater than half the number of votes labeled dissatisfaction, its corresponding raw underwater image is treated as a challenging image and the reference image is discarded. We totally achieve 890 available reference images which have higher quality than any individual methods and a challenging set including 60 underwater images. To visualize the process of reference image generation, we present some cases that the results of some methods are shown and indicate which one is the final reference image in Fig. 4. Furthermore, the percentage of the reference images from the results of different methods is present in Table I. In this paper, we highlight the top 1 performance in red, whereas the second top one is in blue.

TABLE I
PERCENTAGE OF THE REFERENCE IMAGES FROM THE RESULTS OF
DIFFERENT METHODS.

Method	Percentage (%)
Fusion-based [29]	24.72
Two-step-based [30]	7.30
Retinex-based [31]	0.22
DCP [33]	2.58
UDCP [35]	0.00
Regression-based [37]	1.80
GDCP [38]	0.34
Red Channel [40]	0.90
Histogram Prior [42]	13.37
Blurriness-based [43]	3.48
MSCNN [53]	0.90
dive+	43.93

In summary, the results with improved contrast and genuine color are most favored by observers while the over/under enhancement, artifacts, and color casts lead to visually unpleasing results. Finally, the constructed UIEBD includes two subsets: 890 raw underwater images with the corresponding high-quality reference images; 60 challenging underwater images. To the best of our knowledge, it is the first real-world underwater image dataset with reference images so

far. We will periodically update the results for noticeable underwater image enhancement methods. The UIEBD has various potential applications, such as performance evaluation and CNN training. We will introduce these two applications in the next sections.

IV. EVALUATION AND DISCUSSION

A comprehensive and fair evaluation of underwater image enhancement methods has long been missing from the literature. Using the constructed UIEBD, we evaluate the state-of-the-art underwater image enhancement methods (*i.e.*, Fusion-based [29], Two-step-based [30], Retinex-based [31], UDCP [35], Regression-based [37], GDCP [38], Red Channel [40], Histogram Prior [42], Blurriness-based [43]) both qualitatively and quantitatively.

A. Qualitative Evaluation

We first extract several underwater images from the UIEBD, and then divide these images into four categories: greenish underwater images, bluish underwater images, shallow water images, and underwater image with limited illumination. The results of different methods and the corresponding reference images are shown in Figs. 5-8. Note that these underwater images cannot cover the entire UIEBD.

In general, the red light first disappears in water because of its longest wavelength, followed by the green light and then the blue light. Such selective attenuation in water results in the greenish or bluish underwater images, such as the raw underwater images in Figs. 5 and 6. Color deviation seriously affects the visual quality of underwater images and is difficult to be removed. As shown in Figs. 5 and 6, Fusion-based [29], Histogram Prior [42], and Regression-based [37] introduce reddish color deviation due to the inaccurate color correction algorithms used in [29], [37] and the histogram distribution prior [42]. Retinex-based [31] well deals with the color deviation, while UDCP [35] and GDCP [38] tend to aggravate the effect of the color casts. Two-step-based [30] can effectively increase the contrast of underwater images. Red Channel [40] and Blurriness-based [43] have the less positive effect on the greenish and bluish underwater images on account of the limitations of the priors used in these methods. In fact, it is

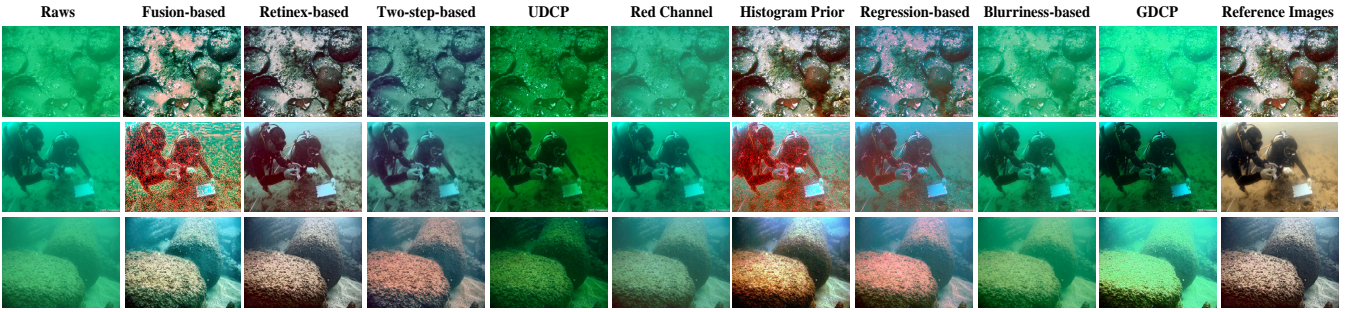


Fig. 5. Subjective comparisons on greenish underwater images. From left to right are raw underwater images, and the results of Fusion-based [29], Retinex-based [31], Two-step-based [30], UDCP [35], Red Channel [40], Histogram Prior [42], Regression-based [37], Blurriness-based [43], GDCP [38], and reference images. **Best viewed with zoom-in on a digital display.**

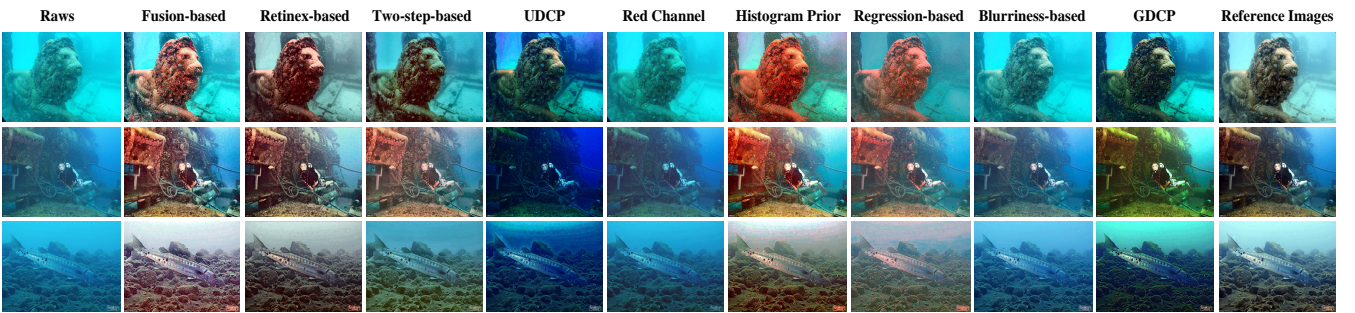


Fig. 6. Subjective comparisons on bluish underwater images. From left to right are raw underwater images, and the results of Fusion-based [29], Retinex-based [31], Two-step-based [30], UDCP [35], Red Channel [40], Histogram Prior [42], Regression-based [37], Blurriness-based [43], GDCP [38], and reference images. **Best viewed with zoom-in on a digital display.**

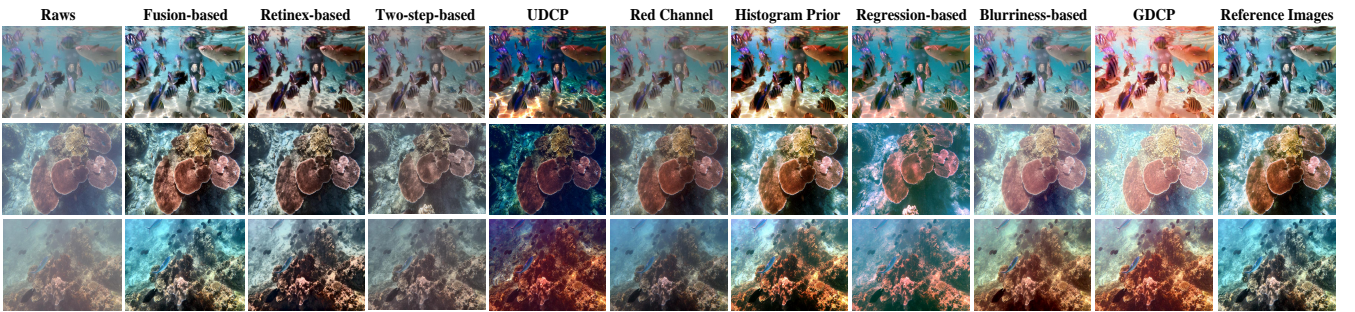


Fig. 7. Subjective comparisons on shallow water images. From left to right are raw underwater images, and the results of Fusion-based [29], Retinex-based [31], Two-step-based [30], UDCP [35], Red Channel [40], Histogram Prior [42], Regression-based [37], Blurriness-based [43], GDCP [38], and reference images. **Best viewed with zoom-in on a digital display.**

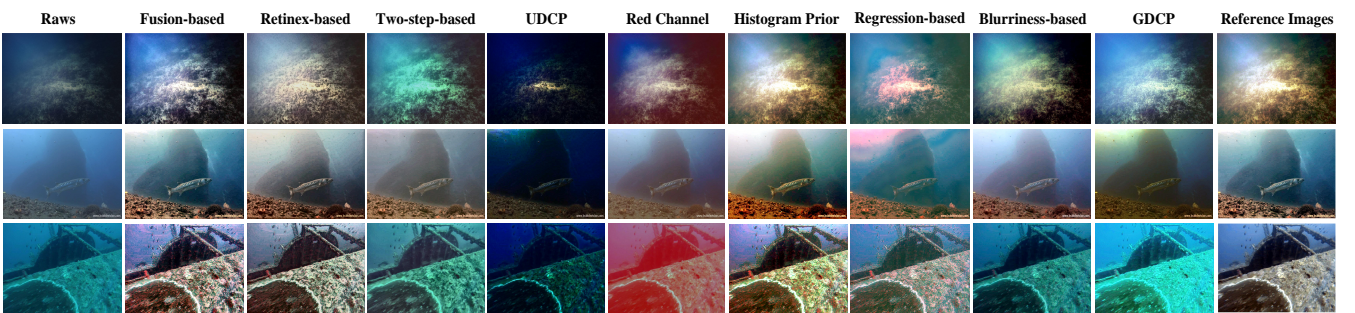


Fig. 8. Subjective comparisons on underwater images with limited illumination. From left to right are raw underwater images, and the results of Fusion-based [29], Retinex-based [31], Two-step-based [30], UDCP [35], Red Channel [40], Histogram Prior [42], Regression-based [37], Blurriness-based [43], GDCP [38], and reference images. **Best viewed with zoom-in on a digital display.**

almost impossible for a color correction algorithm or a kind of prior effective for all types of underwater images.

Images taken in shallow water usually have sufficient illumination as shown in Fig. 7. The methods such as Fusion-based [29], Retinex-based [31], Histogram Prior [42], Regression-based [37], and Blurriness-based [43] significantly remove the effect of haze on the underwater images while UDCP [35] and GDPC [38] bring in obvious color deviation. Two-step-based [30] and Red Channel [40] leave the haze on the results. Compared to other results, the enhanced images by the Fusion-based [29] are visually pleasing.

Different from shallow water images, the images with limited illumination look dark. Generally, such underwater images are hard to be enhanced or recovered. In Fig. 8, Fusion-based [29] and Histogram Prior [42] significantly increase the brightness and contrast of underwater images, which benefits from the histogram modification strategy used in these two methods.

In summary, Fusion-based method [29] has relatively good performance on a variety of underwater images. UDCP [35] tends to produce artifacts on enhanced results in some cases. The other compared methods are effective to some extent.

B. Quantitative Evaluation

To quantitatively evaluate the performance of different methods, we perform the full-reference evaluation, non-reference evaluation, and running time evaluation.

1) *Full-reference Evaluation*: We first conduct a full-reference evaluation using three commonly-used metrics (*i.e.*, MSE, PSNR, and SSIM). We treat the reference images as “ground truth”. The results of full-reference image quality evaluation can provide realistic feedback of the performance of different methods to some extent, although the real ground truth might be different from the reference images. A higher PSNR score and a lower MSE score denote the result is closer to the reference image in terms of image content, while a higher SSIM score means the result is more similar to the reference image in terms of image structure and texture. We present the average scores of different methods on the 890 images with reference images in the UIEBD. As shown in Table II, Fusion-based [29] stands out as the best performer across all metrics. In addition, Two-step-based [30] rank the second best in terms of the full-reference metrics.

TABLE II

FULL-REFERENCE IMAGE QUALITY ASSESSMENT IN TERMS OF MSE, PSNR, AND SSIM.

Method	MSE ($\times 10^3$)	PSNR (dB)	SSIM
Fusion-based [29]	0.8679	18.7461	0.8162
Two-step-based [30]	1.1146	17.6596	0.7199
Retinex-based [31]	1.3351	16.8757	0.6233
UDCP [35]	5.1300	11.0296	0.4999
Regression-based [37]	1.1365	17.5751	0.6543
GDPC [38]	3.6345	12.5264	0.5503
Red Channel [40]	2.1073	14.8935	0.5973
Histogram Prior [42]	1.6282	16.0137	0.5888
Blurriness-based [43]	1.5826	16.1371	0.6582

2) *Non-reference Evaluation*: We employ two non-reference metrics (*i.e.*, UCIQE [62] and UIQM [63]) which are usually used for underwater image quality evaluation [37], [38], [42], [43]. A higher UCIQE score indicates the result has better balance among the chroma, saturation, and contrast, while a higher UIQM score indicates the result is more consistent with the human visual perception. The average scores are shown in Table III.

TABLE III
NO-REFERENCE IMAGE QUALITY EVALUATION IN TERMS OF UCIQE AND UIQM.

Method	UCIQE [62]	UIQM [63]
Fusion-based [29]	0.6414	1.5310
Two-step-based [30]	0.5776	1.4002
Retinex-based [31]	0.6026	1.4338
UDCP [35]	0.5852	1.6297
Regression-based [37]	0.5971	1.2996
GDPC [38]	0.5993	1.4301
Red Channel [40]	0.5421	1.2147
Histogram Prior [42]	0.6778	1.5440
Blurriness-based [43]	0.6001	1.3757

In Table III, Histogram Prior [42] and UDCP [35] obtain the highest scores of UCIQE and UIQM, respectively. It is interesting that the good performers in terms of UCIQE and UIQM metrics are not consistent with the subjective pair comparisons, though both UCIQE and UIQM claim that they take the human visual perception into account. In addition, Figs. 5-8 show the results generated by Histogram Prior [42] and UDCP [35] still suffer from color casts and over-enhancement, and are not as good as those of Fusion-based [29]. Through further analyzing, we found these two non-reference metrics (*i.e.*, UCIQE and UIQM) might be biased to some characteristics (not entire image) and did not take the color shift and artifacts into account. For example, the results with high contrast (*e.g.*, the results of Histogram Prior [42]) are usually favored by the UICQE metric. To illustrate this phenomenon, we present an example in Fig. 9.

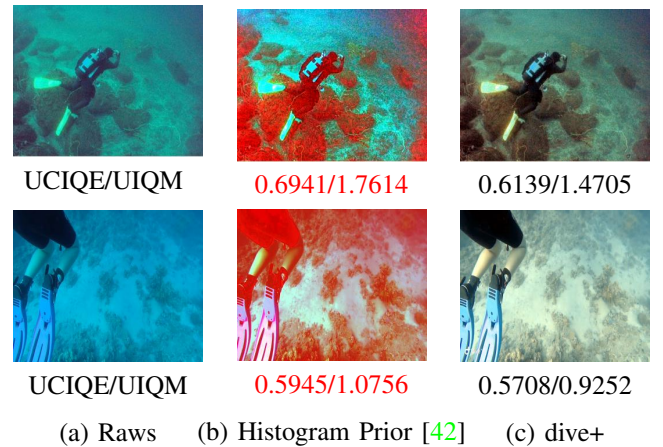


Fig. 9. Visual comparisons in terms of UCIQE and UIQM metrics. From (a) to (c) are the raw underwater images, the results of Histogram Prior [42] and dive+. Higher scores are in red. It is obvious that higher quantitative scores do not lead to better subjectively quality.

In Fig. 9, the results generated by Histogram Prior [42] have obvious reddish color shift and artifacts; however, they

obtain better quantitative scores in terms of UCIQE and UIQM metrics than the results of dive+. Thus, we believe there is a gap between the quantitative scores of non-reference metrics and the subjectively visual quality. In other words, the current image quality evaluation metrics designed for the underwater image have limitations in some cases.

3) *Running Time Evaluation*: We compare the average running time of different methods for the images of different sizes. Experiments are conducted using MATLAB R2014b on a PC with an Intel(R) i7-6700 CPU, 32GB RAM. The average running time is shown in Table IV. Two-step-based [30] is the fastest across different image sizes, while Retinex-based [31] ranks the second fastest. Regression-based [37] is the slowest method due to the time-consuming random forest-based transmission prediction, especially for images with large sizes, which limits its promising applications.

TABLE IV
AVERAGE RUNNING TIME FOR DIFFERENT IMAGE SIZES (SECONDS).

Method	500 × 500	640 × 480	1280 × 720
Fusion-based [29]	0.6044	0.6798	1.8431
Two-step-based [30]	0.2978	0.4391	1.0361
Retinex-based [31]	0.6975	0.8829	2.1089
UDCP [35]	2.2688	3.3185	9.9019
Regression-based [37]	138.6138	167.1711	415.4935
GDCP [38]	3.2676	3.8974	9.5934
Red Channel [40]	2.7523	3.2503	9.7447
Histogram Prior [42]	4.6284	5.8289	16.9229
Blurriness-based [43]	37.0018	47.2538	146.0233

After reviewing and evaluating the state-of-the-art underwater image enhancement methods, we found that Fusion-based [29] is the relatively best performer in most cases, while other compared methods have obvious disadvantages. However, there is no method which always wins when facing a large-scale real-world underwater image dataset (*i.e.*, UIEBD). All in all, due to neglecting the underwater imaging physical models, the non-physical model-based methods, such as Two-step-based [30] and Retinex-based [31], produce over-enhanced or under-enhanced results. Physical model-based methods such as UDCP [35] employ an outdoor haze formation based model to predict the medium transmission which is not well-suited for the underwater scenario. Inaccurate physical models and assumptions result in color casts and remaining haze in the results of physical model-based methods such as Regression-based [37], GDCP [38], Red Channel [40], Histogram Prior [42], and Blurriness-based [43]. Some methods such as Retinex-based [31] and Histogram Prior [42] tend to introduce noise and artifacts, which leads to visually unpleasing results. The running time of some methods seriously limits their practical applications.

In the future, a comprehensive method that can robustly deal with a variety of underwater image degradation is expected. The non-reference metrics which are more effective and consistent with human visual perception are desired in the community of underwater image enhancement.

V. PROPOSED MODEL

Despite the remarkable progress of underwater image enhancement methods, the generalization of deep learning-based underwater image enhancement models still falls behind the conventional state-of-the-art methods due to the lack of effective training data and well-designed network architectures for underwater image enhancement. With the constructed UIEBD, we propose a CNN model for underwater image enhancement, called DUIENet. The purpose of the proposed DUIENet as a baseline is to call for the development of deep learning-based underwater image enhancement, and demonstrate the generalization of the constructed UIEBD for training CNN. Note that the proposed DUIENet is only a baseline model which can be further improved by well-designed network architectures, task-related loss functions, and the like.

In this section, we first present input generation from an underwater image and the architecture of the proposed DUIENet. Then we present the training and implementation details. At last, we perform experiments to demonstrate the advantage of the proposed DUIENet. All the source code of the proposed deep model will be made available to the public.

A. Input Generation

As discussed in Section IV, there is no algorithm generalized to all types of underwater images due to the complicated underwater environment and lighting conditions. In general, the Fusion-based method [29] achieves decent results, which benefits from the inputs derived by multiple pre-processing operations and a fusion strategy. In the proposed DUIENet, we also employ such a manner. Based on the characteristics of underwater image degradation, we generate three inputs by respectively applying White Balance (WB), Histogram Equalization (HE) and Gamma Correction (GC) algorithms to an underwater image. Specifically, WB algorithm is used to correct the color casts of an underwater image, while HE and GC algorithms aim to improve the contrast and light up dark regions, respectively. We directly employ the WB algorithm in [29], whose effectiveness has been turned out. For the HE algorithm, we apply the *adapthisteq* function [70] provided by MATLAB to the L component in Lab color space, and then transform back into RGB color space. We set the gamma value of GC algorithm as 0.7 empirically.

B. Network Architecture

DUIENet employs a gated fusion network architecture to learn three confidence maps which will be used to combine the three input images into an enhanced result. The learned confidence maps determine the most significant features of inputs remaining in the final result. Gated fusion network architecture has not been explored in the context of underwater image enhancement. In addition, the impressive performance of the fusion-based underwater image enhancement method [29] also encourages us to explore the fusion-based networks.

The architecture of the proposed DUIENet and parameter settings are shown in Fig. 10. As a baseline model, the proposed DUIENet is a plain fully CNN. We believe that the

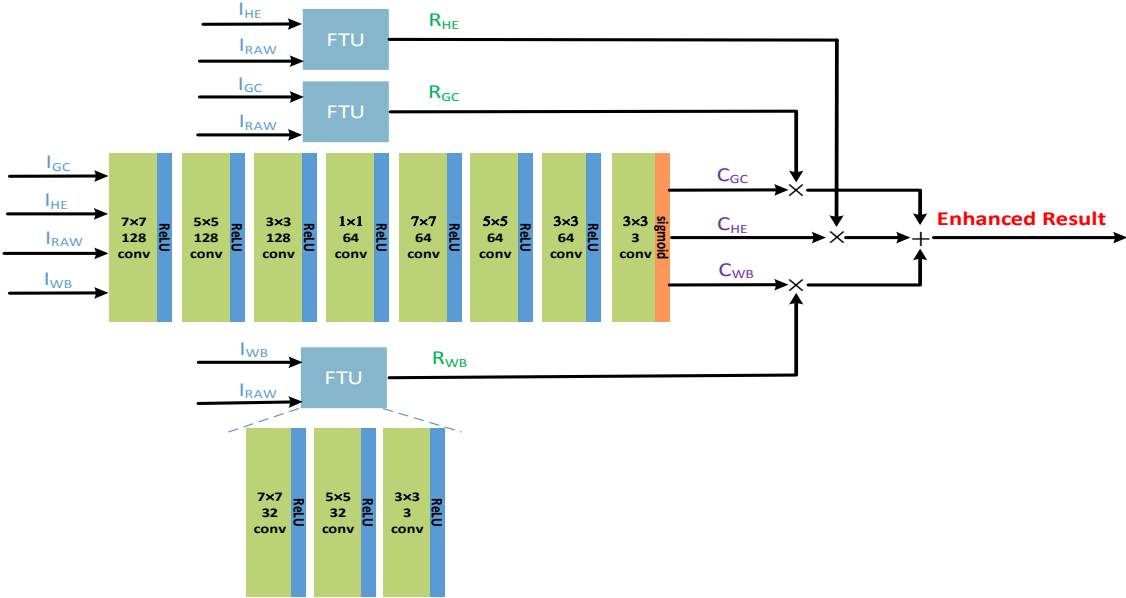


Fig. 10. An overview of the proposed DuwieNet architecture. DuwieNet is a gated fusion network, which fuses the inputs with the predicted confidence maps to achieve the enhanced result. The inputs are first transferred to the refined inputs by the FTUs and then confidence maps are predicted. At last, the enhanced result is achieved by fusing the refined inputs and the corresponding confidence maps.

widely used backbones such as the U-Net architecture [71] and the residual network architecture [72] can be incorporated to improve the performance. We leave it as the future work. We feed the three derived inputs and original input to the proposed DUIENet to predict the confidence maps. Before performing fusion, we add three Feature Transformation Units (FTUs) to refine the three inputs. The purpose of the FTU is to reduce the color casts and artifacts introduced by the WB, HE, and GC algorithms. At last, the refined three inputs are multiplied by the three learned confidence maps to achieve the final enhanced result:

$$I_{en} = R_{WB} \odot C_{WB} + R_{HE} \odot C_{HE} + R_{GC} \odot C_{GC}, \quad (1)$$

where I_{en} is the final enhanced result; \odot indicates the element-wise product of matrices; R_{WB} , R_{HE} , and R_{GC} are the refined results of input after processing by WB, HE, and GC algorithms, respectively; C_{WB} , C_{HE} , and C_{GC} are the learned confidence maps.

C. Implementation

A random set of 800 pairs of the images extracted from the constructed UIEBD is used to generate the training set. We resize the input images to size 112×112 due to our limited memory. Flipping and rotation are used to obtain 7 additional augmented versions of original training data. The rest 90 pairs of the images in the UIEBD dataset are treated as the testing set. To reduce the artifacts induced by pixel-wise loss functions such as ℓ_1 and ℓ_2 , we minimize the perceptual loss function to learn the mapping function of underwater image enhancement. Inspired by [73], we define the perceptual loss based on the ReLU activation layers (*i.e.*, layer `relu5_4`) of the pre-trained 19 layers VGG network [74]. Let $\phi_j(x)$ be the j th convolutional layer (after activation) of the VGG19 network ϕ

pretrained on the ImageNet dataset [75]. The perceptual loss is expressed as the distance between the feature representations of the enhanced image I_{en} and the reference image I_{gt} :

$$L_j^\phi = \frac{1}{C_j H_j W_j} \sum_{i=1}^N \| \phi_j(I_{en}^i) - \phi_j(I_{gt}^i) \|, \quad (2)$$

where N is the number of each batch in the training procedure; $C_j H_j W_j$ represents the dimension of the feature maps of the j th convolutional layer within the VGG19 network. C_j , H_j , and W_j are the number, height, and width of the feature map, respectively.

We implemented the proposed DUIENet with TensorFlow on a PC with an Intel(R) i7 6700 CPU, 32GB RAM, and an NVIDIA GeForce GTX 1080Ti GPU. During training, a batch-mode learning method with a batch size of 16 was applied. The filter weights of each layer were initialized by ‘‘Xavier’’ [76]. Bias was initialized as a constant. We used ADAM [77] with default parameters for our network optimization. We initialized the learning rate to $1e^{-3}$ and decreased the learning rate by 0.1 every 10,000 iterations until the proposed DUIENet converges. The training for the proposed DUIENet with aforementioned parameter settings took roughly 6 hours. With an NVIDIA GTX 1080Ti GPU, the proposed DUIENet can process an image with a size of 640×480 within 0.128s (8FPS), which is very fast in practical applications.

D. Experiments

To demonstrate the advantages achieved by the proposed DUIENet, we compare it against five state-of-the-art underwater image enhancement methods. The experiments are conducted on the testing set which includes 90 underwater images and the challenging set including 60 underwater images. We show several results in Figs. 11 and 12.

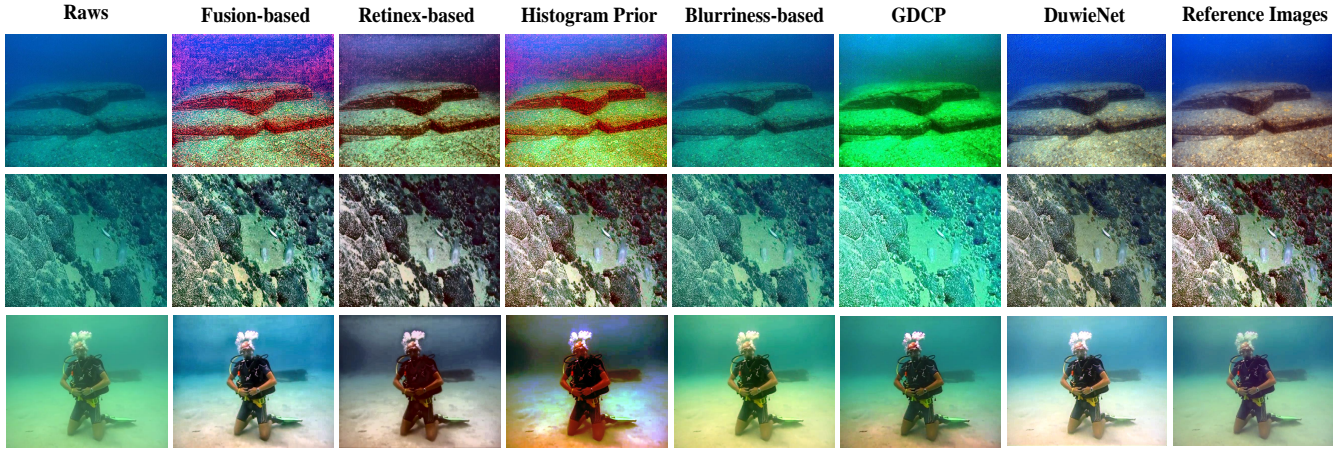


Fig. 11. Subjective comparisons on underwater images from testing set. From left to right are raw underwater images, and the results of Fusion-based [29], Retinex-based [31], Histogram Prior [42], Blurriness-based [43], GDCP [38], the proposed DuvieNet, and reference images.

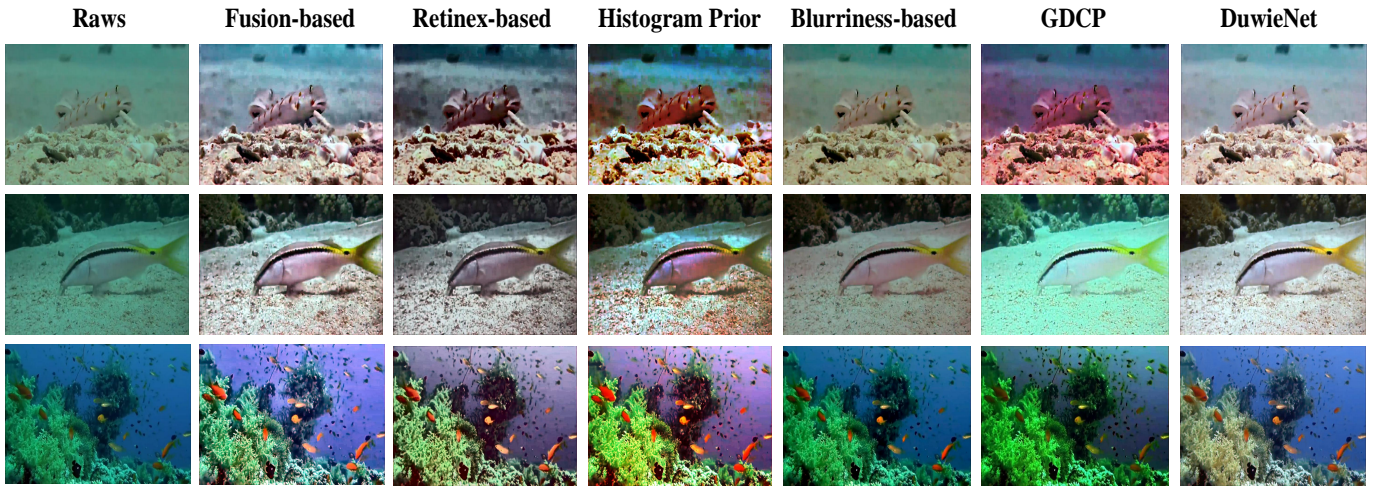


Fig. 12. Subjective comparisons on underwater images from challenging set. From left to right are raw underwater images, and the results of Fusion-based [29], Retinex-based [31], Histogram Prior [42], Blurriness-based [43], GDCP [38], and the proposed DuvieNet.

As shown in Fig. 11, the proposed DUIENet effectively removes the haze on the underwater images and remits color casts, while the compared methods introduce unexpected colors (*e.g.*, Fusion-based [29], GDCP [38], and Histogram Prior [42]) and artifacts (*e.g.*, Fusion-based [29], Retinex-based [31], and Histogram Prior [42]) or have little effect on inputs (*e.g.*, Blurriness-based [43]). In addition, it is interesting that our results even achieve better visual quality than the corresponding reference images (*e.g.*, less noise and better details). This is because that the perceptual loss-based DUIENet can learn the potential attributes of good visual quality from the constructed large-scale real-world underwater image dataset. For the results of different methods on challenging set shown in Fig. 12, the proposed DUIENet produces visually pleasing results. By contrast, other methods tend to introduce artifacts, over-enhancement (*e.g.*, the backgrounds and the foregrounds), and color casts (*e.g.*, the reddish or greenish color).

Table V reports the quantitative results of different methods in terms of MSE, PSNR, and SSIM on the testing set. The

TABLE V
FULL-REFERENCE IMAGE QUALITY ASSESSMENT IN TERMS OF MSE, PSNR, AND SSIM ON TESTING SET.

Method	MSE ($\times 10^3$)	PSNR (dB)	SSIM
Fusion-based [29]	1.1280	17.6077	0.7721
Retinex-based [31]	1.2924	17.0168	0.6071
GDCP [38]	4.0160	12.0929	0.5121
Histogram Prior [42]	1.7019	15.8215	0.5396
Blurriness-based [43]	1.9111	15.3180	0.6029
DuvieNet	0.7976	19.1130	0.7971

quantitative results are obtained by comparing the results of each method with the corresponding reference image. We discard the non-reference metrics designed for underwater image enhancement based on the conclusion presented in Sec. IV. Our method achieves the best performance in terms of full-reference image quality assessment. In addition, instead of pairwise comparison, we conduct a user study to score the visual quality of the results on challenging set. This is because some images in the challenging set are too difficult to

obtain satisfactory results following the procedure of reference image generation. Thus, we invited 50 participants (the same volunteers with the reference image generation) to score results. The scores have five scales ranging from 5 to 1 which represent “Excellent”, “Good”, “Fair”, “Poor” and “Bad”, respectively. The average scores of the results by each method on challenging set are shown in Table VI. Besides, we also provide the standard deviation of the results by each method on challenging set. Our method receives the highest average score and lowest standard deviation, which indicates our method produces better results from a subjective perspective and has more robust performance than several state-of-the-art methods.

TABLE VI
THE AVERAGE SCORES AND STANDARD DEVIATION OF DIFFERENT METHODS ON CHALLENGING SET.

Method	Average Score	Standard Deviation
Fusion-based [29]	2.28	0.8475
Retinex-based [31]	2.23	0.8720
GDCP [38]	1.90	0.8099
Histogram Prior [42]	2.08	0.7897
Blurriness-based [43]	2.02	0.7762
DuwieNet	2.57	0.7280

Qualitative and quantitative experiments demonstrate the effectiveness of the proposed DUIENet and also indicate the constructed dataset can be used for training CNN. However, there is still room for the improvement of underwater image enhancement. In addition, underwater images in the challenging set still cannot be enhanced well. We look forward to more effective and efficient methods.

VI. CONCLUSION AND FUTURE WORK

In this paper, we have constructed an underwater image enhancement benchmark dataset which offers large-scale degraded underwater images and the corresponding reference images. This benchmark dataset enables us to comprehensively study the existing underwater image enhancement methods, and easily train CNN for underwater image enhancement. As analyzed in qualitative and quantitative evaluations, there is no method which always wins in terms of full- and no-reference metrics. In other words, there is still much room for the improvement of underwater image enhancement. In addition, effective non-reference underwater image quality evaluation metrics are highly desirable. To promote the development of deep learning-based underwater image enhancement methods, we proposed an underwater image enhancement CNN model trained by the constructed dataset. Experimental results demonstrate the proposed CNN model performs favorably against the state-of-the-art methods, and also verify the generalization of the constructed dataset for training CNN. In the future work, we will extend the constructed dataset towards more challenging underwater images and underwater videos. Moreover, we tend to investigate more effective underwater image enhancement CNN models which take advantages of the prior information of underwater imaging.

REFERENCES

- J. Jaffe, “Underwater optical imaging: The past, the present, and the prospects,” *IEEE J. Oceanic Eng.*, vol. 40, no. 3, pp. 683-700, 2015. [1](#)
- M. Sheinin and Y. Schechner, “The next best underwater view,” in *Proc. of IEEE Int. Conf. Comput. Vis. Pattern Rec. (CVPR)*, 2016, pp. 3764-3773. [1](#)
- B. McGlamery, “A computer model for underwater camera systems,” in *Ocean Optics VI*, pp. 221-231, 1980. [1](#)
- J. Jaffe, “Computer modeling and the design of optimal underwater imaging systems,” *IEEE J. Oceanic Eng.*, vol. 15, no. 2, pp. 101-111, 1990. [1](#)
- W. Hou, S. Woods, E. Jarosz, *et al.*, “Optical turbulence on underwater image degradation in natural environments,” *Appl. Opt.*, vol. 15, no. 14, pp. 2678-2686, 2012. [1](#)
- D. Akkaynak and T. Treibitz, “A revised underwater image formation model,” in *Proc. of IEEE Int. Conf. Comput. Vis. Pattern Rec. (CVPR)*, 2017, pp. 6723-6732. [1](#)
- D. Akkaynak, T. Treibitz, T. Shlesinger, *et al.*, “What is the space of attenuation coefficients in underwater computer vision,” in *Proc. of IEEE Int. Conf. Comput. Vis. Pattern Rec. (CVPR)*, 2017, pp. 568-577. [1](#)
- M. Ludvigsen, B. Sortland, G. Johnsen, *et al.*, “Applications of georeferenced underwater photo mosaics in marine biology and archaeology,” *J. Oceanography*, vol. 20, no. 4, pp. 140-149, 2007. [1](#)
- N. Strachan, “Recognition of fish species by colour and shape,” *J. Image Vis. Comput.*, vol. 11, no. 1, pp. 2-10, 1993. [1](#)
- Y. LeCun, Y. Bengio, and G. Hinton, “Deep learning,” *Nature*, vol. 521, no. 7553, pp. 436-444, 2015. [1](#)
- K. He, X. Zhang, S. Ren, *et al.*, “Deep residual learning for image recognition,” in *Proc. of IEEE Int. Conf. Comput. Vis. Pattern Rec. (CVPR)*, 2016, pp. 770-778. [1](#)
- R. Li, K. Li, Y. C, *et al.*, “Referring image segmentation via recurrent refinement networks,” in *Proc. of IEEE Int. Conf. Comput. Vis. Pattern Rec. (CVPR)*, 2018, pp. 5745-5753. [1](#)
- K. Zhang, W. Zuo, and S. Gu, “Learning deep CNN denoiser prior for image restoration,” in *Proc. of IEEE Int. Conf. Comput. Vis. Pattern Rec. (CVPR)*, 2017, pp. 2808-2817. [1](#)
- R. Schettini and S. Corchs, “Underwater image processing: State of the art of restoration and image enhancement methods,” *J. Advan. Signal Process.*, vol. 2010, pp. 1-14, 2010. [2](#)
- M. Han, Z. Lyu, and T. Qiu, “A review on intelligence dehazing and color restoration for underwater images,” *IEEE Trans. Syst., Man, Cybern.*, Syst., pp. 1-13, 2018 (Early Access). [2](#)
- R. Cui, L. Chen, C. Yang, *et al.*, “Extended state observer-based integral sliding mode control for an underwater robot with unknown disturbances and uncertain nonlinearities,” *IEEE Trans. Ind. Electron.*, vol. 64, no. 8, pp. 6785-6795, 2017. [2](#)
- S. Narasimhan and S. Nayar, “Contrast restoration of weather degraded images,” *IEEE Trans. Pattern Anal. Mach. Intell.*, vol. 25 no. 6, pp. 713-724, 2003. [2](#)
- N. Sharshar, R. Hanlon, and A. deM. Petz, “Polarization vision helps detect transparent prey,” *Nature*, vol. 393 no. 6682, pp. 222-223, 1998. [2](#)
- Y. Schechner and N. Karpel, “Clear underwater vision,” in *Proc. of IEEE Int. Conf. Comput. Vis. Pattern Rec. (CVPR)*, 2004, pp. 536-543. [2](#)
- Y. Schechner and N. Karpel, “Recovery of underwater visibility and structure by polarization analysis,” *IEEE J. Oceanic Eng.*, vol. 30, no. 3, pp. 570-587, 2005. [2](#)
- T. Treibitz and Y. Schechner, “Active polarization descattering,” *IEEE Trans. Pattern Anal. Mach. Intell.*, vol. 31, no. 3, pp. 385-399, 2009. [2](#)
- C. Tan, G. Sluzek, and D. He, “A novel applications of range-gated underwater laser imaging system in near target turbid medium,” *Optics and Lasers Eng.*, vol. 43, no. 9, pp. 995-1009, 2005. [2](#)
- H. Li, X. Wang, T. Bai, *et al.*, “Speckle noise suppression of range gated underwater imaging system,” *Applid Optics*, vol. 38, no. 18, pp. 3937-3944, 2009. [2](#)
- T. Treibitz and Y. Schechner, “Turbid scene enhancement using multi-directional illumination fusion,” *IEEE Trans. Image Process.*, vol. 21, no. 11, pp. 4662-4667, 2012. [2](#)
- Z. Murez, T. Treibitz, R. Ramamoorthi, *et al.*, “Photometric stereo in a scattering medium,” in *Proc. of IEEE Int. Conf. Comput. Vis. Pattern Rec. (CVPR)*, 2015, pp. 3415-3423. [2](#)
- K. Iqbal, M. Odetayo, and A. James, “Enhancing the low quality images using unsupervised colour correction method,” in *Proc. of IEEE Int. Conf. Syst., Man, Cybern.*, 2010, pp. 1703-1709. [2](#)
- A. Ghani and N. Isa, “Underwater image quality enhancement through integrated color model with Rayleigh distribution,” *Appl. Soft Comput.*, vol. 27, pp. 219-230, 2015. [2](#)
- A. Ghani and N. Isa, “Enhancement of low quality underwater image through integrated global and local contrast correction,” *Appl. Soft Comput.*, vol. 37, pp. 332-344, 2015. [2](#)

[29] C. Ancuti, C. O. Ancuti, and P. Bekaert, "Enhancing underwater images and videos by fusion," in *Proc. of IEEE Int. Conf. Comput. Vis. Pattern Rec. (CVPR)*, 2012, pp. 81-88. [2](#), [4](#), [5](#), [6](#), [7](#), [8](#), [10](#), [11](#)

[30] X. Fu, Z. Fan, and M. Ling, "Two-step approach for single underwater image enhancement," in *Symposium. of IEEE Intell. Signal Process. Commun. Syst.*, 2017, pp. 789-794. [2](#), [4](#), [5](#), [6](#), [7](#), [8](#)

[31] X. Fu, P. Zhang, Y. Huang, *et al.*, "A retinex-based enhancing approach for single underwater image," in *Proc. of IEEE Int. Conf. Image Process. (ICIP)*, 2014, pp. 4572-4576. [2](#), [4](#), [5](#), [6](#), [7](#), [8](#), [10](#), [11](#)

[32] S. Zhang, T. Wang, J. Dong, *et al.*, "Underwater image enhancement via extended multi-scale Retinex," *Neurocomput.*, vol. 245, no. 5, pp. 1-9, 2017. [2](#)

[33] K. He, J. Sun, and X. Tang, "Single image haze removal using dark channel prior," *IEEE Trans. Pattern Anal. Mach. Intell.*, vol. 33, no. 12, pp. 2341-2353, 2011. [2](#), [4](#), [5](#)

[34] J. Chiang and Y. Chen, "Underwater image enhancement by wavelength compensation and dehazing," *IEEE Trans. Image Process.*, vol. 21, no. 4, pp. 1756-1769, 2012. [2](#)

[35] P. Drews-Jr, E. Nascimento, S. Botelho, *et al.*, "Underwater depth estimation and image restoration based on single images," *IEEE Comput. Graph. Appl.*, vol. 36, no. 2, pp. 24-35, 2016. [2](#), [4](#), [5](#), [6](#), [7](#), [8](#)

[36] H. Liu and L. Chau, "Underwater image restoration based on contrast enhancement," in *Proc. of IEEE Int. Digit. Signal Process.*, 2016, pp. 584-588. [2](#)

[37] C. Li, J. Guo, C. Guo, *et al.*, "A hybrid method for underwater image correction," *Pattern Rec. Lett.*, vol. 94, pp. 62-67, 2017. [2](#), [4](#), [5](#), [6](#), [7](#), [8](#)

[38] Y. Peng, T. Cao, and P. Cosman, "Generalization of the dark channel prior for single image restoration," *IEEE Trans. Image Process.*, vol. 27, no. 6, pp. 2856-2868, 2018. [2](#), [4](#), [5](#), [6](#), [7](#), [8](#), [10](#), [11](#)

[39] N. Carlevaris-Bianco, A. Mohan, and R. Eustice, "Initial results in underwater single image dehazing," in *Proc. of IEEE Int. Conf. Oceans*, 2010, pp. 1-8. [2](#)

[40] A. Galdran, D. Pardo, and A. Picn, "Automatic Red-Channel underwater image restoration," *J. Vis. Commu. and Image Repr.*, vol. 26, pp. 132-145, 2015. [3](#), [4](#), [5](#), [6](#), [7](#), [8](#)

[41] X. Zhao, T. Jin, and S. Qu, "Deriving inherent optical properties from background color and underwater image enhancement," *Ocean Eng.*, vol. 94, pp. 163-172, 2015. [3](#)

[42] C. Li, J. Guo, R. Cong, *et al.*, "Underwater image enhancement by dehazing with minimum information loss and histogram distribution prior," *IEEE Trans. Image Process.*, vol. 25, no. 12, pp. 5664-5677, 2016. [3](#), [4](#), [5](#), [6](#), [7](#), [8](#), [10](#), [11](#)

[43] Y. Peng and P. Cosman, "Underwater image restoration based on image blurriness and light absorption," *IEEE Trans. Image Process.*, vol. 26, no. 4, pp. 1579-1594, 2017. [3](#), [4](#), [5](#), [6](#), [7](#), [8](#), [10](#), [11](#)

[44] D. Berman, T. Treibitz, and S. Avidan, "Diving into Haze-lines: Color restoration of underwater images," in *Proc. of Briti. Mach. Vis. Conf. (BMVC)*, 2017, pp. 1-12. [3](#)

[45] Y. Wang, H. Liu, and L. Chau, "Single underwater image restoration using adaptive attenuation-curve prior," *IEEE Trans. Circuits Syst. I, Reg. Papers*, vol. 65, no. 3, pp. 992-1002, 2018. [3](#)

[46] C. Dong, C. Loy, K. He, *et al.*, "Learning a deep convolutional network for image super-resolution," in *Proc. of Eur. Conf. Comput. Vis. (ECCV)*, 2014, pp. 184-199. [3](#)

[47] C. Dong, C. Loy, K. He, *et al.*, "Image super-resolution using deep convolutional networks," *IEEE Trans. Pattern Anal. Mach. Intell.*, vol. 38 no. 2, pp. 295-307, 2016. [3](#)

[48] W. Lai, J. Huang, N. Ahuja, *et al.*, "Deep laplacian pyramid network for fast and accurate superresolution," in *Proc. of IEEE Int. Conf. Comput. Vis. Pattern Rec. (CVPR)*, 2017, pp. 624-632. [3](#)

[49] X. Mao, C. Shen, and Y. Yang, "Image restoration using very deep convolutional encoder-decoder networks with symmetric skip connections," in *Proc. of Advances Neural Inf. Process. Syst. (NeurIPS)*, 2016, pp. 2802-2810. [3](#)

[50] K. Zhang, W. Zuo, Y. Chen, *et al.*, "Beyond a gaussian denoiser: Residual learning of deep cnn for image denoising," *IEEE Trans. Image Process.*, vol. 26, no. 7, pp. 3142-3155, 2017. [3](#)

[51] L. Li, J. Pan, W. Lai, *et al.*, "Learning a discriminative prior for blind image blurring," in *Proc. of IEEE Int. Conf. Comput. Vis. Pattern Rec. (CVPR)*, 2018, pp. 6616-6625. [3](#)

[52] J. Zhang, J. Pan, J. Ren, *et al.*, "Dynamic scene deblurring using spatially variant recurrent neural networks," in *Proc. of IEEE Int. Conf. Comput. Vis. Pattern Rec. (CVPR)*, 2018, pp. 2521-2529. [3](#)

[53] W. Ren, S. Liu, H. Zhang, *et al.*, "Single image dehazing via multi-scale convolutional neural networks," in *Proc. of Eur. Conf. Comput. Vis. (ECCV)*, 2016, pp. 154-169. [3](#), [4](#), [5](#)

[54] B. Li, X. Peng, Z. Wang, "All-in-one dehazing network," in *Proc. of IEEE Int. Conf. Comput. Vis. (ICCV)*, 2017, pp. 4770-4778. [3](#)

[55] J. Li, K. Sinner, R. Eustice, *et al.*, "WaterGAN: Unsupervised generative network to enable real-time color correction of monocular underwater images," *IEEE Robot. Autom. Lett.*, vol. 3, no. 1, pp. 387-394, 2018. [3](#), [4](#)

[56] C. Li, J. Guo, and C. Guo, "Emerging from water: Underwater image color correction based on weakly supervised color transfer," *IEEE Signal Process. Lett.*, vol. 25, no. 3, pp. 323-327, 2018. [3](#)

[57] Y. Zhu, T. Par, P. Isola, *et al.*, "Unpaired image-to-image translation using cycle-consistent adversarial networks," in *Proc. of IEEE Int. Conf. Comput. Vis. (ICCV)*, 2017, pp. 2242-2251. [3](#)

[58] M. Hou, R. Liu, X. Fan, *et al.*, "Joint residual learning for underwater image enhancement," in *Proc. of IEEE Int. Conf. Image Process. (ICIP)*, 2018, pp. 4043-4047. [3](#)

[59] Z. Wang, A. Bovik, H. Sheikh, *et al.*, "Image quality assessment: From error visibility to structural similarity," *IEEE Trans. Image Process.*, vol. 13, no. 4, pp. 600-612, 2004. [3](#)

[60] N. Hautiere, J. Tarel, D. Aubert, *et al.*, "Blind contrast enhancement assessment by gradient ratioing at visible edges," *Image Anal. Stereo.*, vol. 27, no. 2, pp. 87-95, 2011. [3](#)

[61] T. Aydin, R. Mantiuk, K. Myszkowski, *et al.*, "Dynamic range independent image quality assessment," *ACM Trans. Graphics*, vol. 27, no. 3, pp. 69-79, 2008. [3](#)

[62] M. Yang and A. Sowmya, "An underwater color image quality evaluation metric," *IEEE Trans. Image Process.*, vol. 24, no. 12, pp. 6062-6071, 2015. [3](#), [7](#)

[63] K. Panetta, C. Gao, and S. Agaian, "Human-visual-system-inspired underwater image quality measures," *IEEE J. Ocean Eng.*, vol. 41, no. 3, pp. 541-551, 2016. [3](#), [7](#)

[64] J. Xiao, J. Hays, K. Ehinger, *et al.*, "Sun database: Large-scale scene recognition from abbey to zoo," in *Proc. of IEEE Int. Conf. Comput. Vis. Pattern Rec. (CVPR)*, 2010, pp. 3485-3492. [3](#)

[65] A. Duarte, F. Codevilla, J. Gaya, *et al.*, "A dataset to evaluate underwater image restoration methods," in *Proc. of IEEE Int. Conf. Oceans*, 2016, pp. 1-6. [4](#)

[66] H. Blasinski, T. Lian, and E. Farrell, "Underwater image systems simulation," in *Imaging and Applied Optics*, 2017, pp. 1-2. [4](#)

[67] H. Blasinski and E. Farrell, "A three parameter underwater image formation model," *Electron. Imag.*, vol. 18, pp. 1-8, 2016. [4](#)

[68] J. Cai, S. Gu, and L. Zhang, "Learning a deep single image contrast enhancer from multi-exposure images," *IEEE Trans. Image Process.*, vol. 27, no. 4, pp. 2049-2062, 2018. [4](#)

[69] B. Li, W. Ren, D. Fu, *et al.*, "Benchmarking single image dehazing and beyond," *IEEE Trans. Image Process.*, vol. 28, no. 1, pp. 492-505, 2019. [4](#)

[70] K. Zuiderveld, "Contrast limited adaptive histogram equalization," *Graphics Gems*, pp. 474-485, 1994. [8](#)

[71] O. Ronneberger, P. Fischer, and T. Brox, "U-Net: Convolutional networks for biomedical image segmentation," in *Proc. of Med. Image Comput. Comput. Assist. Inter. (MICCAI)*, 2015, pp. 234-241. [9](#)

[72] K. He, X. Zhang, S. Ren, *et al.*, "Deep residual learning for image recognition," in *Proc. of IEEE Int. Conf. Comput. Vis. Pattern Rec. (CVPR)*, 2016, pp. 770-778. [9](#)

[73] J. Johnson, A. Alahi, and L. Fei-Fei, "Perceptual losses for real-time style transfer and super-resolution," in *Proc. of Eur. Conf. Comput. Vis. (ECCV)*, 2016, pp. 694-711. [9](#)

[74] K. Simonyan and A. Zisserman, "Very deep convolutional networks for large-scale image recognition," in *Proc. of Int. Conf. Machine Learn. (ICML)*, 2015, pp. 1-14. [9](#)

[75] J. Deng, W. Dong, R. Socher, *et al.*, "Imagenet: A large-scale hierarchical image database," in *Proc. of IEEE Int. Conf. Comput. Vis. Pattern Rec. (CVPR)*, 2009, pp. 248-255. [9](#)

[76] X. Glorot and Y. Bengio, "Understanding the difficulty of training deep feedforward neural networks," in *Proc. of Int. Conf. Art. Intell. Stat.*, 2010, pp. 249-256. [9](#)

[77] D. Kingma and J. Ba, "Adam: A method for stochastic optimization," in *arXiv preprint arXiv: 1412.6980*, 2017. [9](#)